

# MOLLEO+: TOWARDS OPTIMIZED USE OF LLMs FOR DRUG DISCOVERY

**Anonymous authors**

Paper under double-blind review

## ABSTRACT

Large language models (LLMs) have recently emerged as a promising tool for small-molecule generation in drug discovery. One notable recent state-of-the-art work in this field is MOLLEO (Wang et al., 2025), which combines an evolutionary algorithm with an LLM that acts as the operator for making crossovers and mutations on the ligand population. MOLLEO demonstrates strong results on optimizing molecular docking scores, but several aspects of their model are not well suited to real-world drug discovery. We introduce MOLLEO+, an optimized LLM workflow for small-molecule generation. First, we replace docking with the recently released biomolecular foundation model Boltz-2 as an oracle, which improves the predicted binding affinity of generated molecules using gold-standard molecular dynamics by over 100%. Second, we incorporate knowledge of existing ligands, which is present in most practical drug discovery scenarios, using ligands from BindingDB instead of ZINC 250k as the starting population for the genetic algorithm. Third, we propose a fine-tuning strategy to better modify existing ligands towards higher activity. We demonstrate the superiority of MOLLEO+ on the receptor tyrosine kinase c-MET and the BRD4 protein, yielding an improvement over state-of-the-art baselines by up to 20% for Boltz-2 binding affinity.

## 1 INTRODUCTION

Large Language Models (LLMs) have recently gained interest for their ability to make significant discoveries and advancements in scientific areas. This is perhaps most notable in the recent AlphaEvo (Altschul et al., 1990), an evolutionary approach that uses LLMs to progressively improve the quality of a generated algorithm. It successfully developed state-of-the-art algorithms for multiple problems in mathematics and computer science.

However, studies on applying LLMs to the field of small-molecule generation for drug discovery have been limited. Most previous work in machine learning for small-molecule drug design has focused on VAEs (Eckmann et al., 2022; 2025; Noh et al., 2022), diffusion models (Lee et al., 2023; Hoogetboom et al., 2022; Zhou et al., 2024), reinforcement learning (Jeon & Kim, 2020; Fu et al., 2022; Mazuz et al., 2023), and other generative frameworks (Zhu et al., 2023). These methods are often guided by a cheap oracle such as AutoDock (Trott & Olson, 2009), which predicts the binding affinity of generated compounds to a particular protein target; however, it is known to be inaccurate in reflecting actual experimental activity (Handa et al., 2023). Thus, most current frameworks struggle with generating compounds that are likely to show experimental binding.

Recently, LLMs have begun to garner interest as a method to generate small molecule binders, showing promise in generating strong, drug-like ligands. In contrast to more specialized models, LLMs hold the distinct advantage of being implicitly aware of how chemistry is typically done (e.g. common reactions, lead optimization techniques, etc.), giving them great potential in problems related to chemical discovery (White, 2023). This has been demonstrated in the notable previous work MOLLEO (Wang et al., 2025), an evolutionary algorithm that incorporates LLMs as a mutation and crossover operator. They report state-of-the-art results for generating molecules with multiple desired properties, demonstrating the potential of LLMs as a generative framework in the field.

In this work, we further advance LLMs for small molecule drug discovery by introducing a set of novel optimizations to improve their real-world effectiveness. We introduce MOLLEO+, an optimized framework specially designed for optimizing protein-ligand binding affinity. First, we replace

054 the AutoDock (Trott & Olson, 2009) oracle in MOLLEO with the new biomolecular foundation  
055 model Boltz-2 (Passaro et al., 2025). We demonstrate that this relatively cheap oracle significantly  
056 improves the quality of generated ligands over AutoDock, as measured by the gold-standard Ab-  
057 solute Binding Free Energy (Feng et al., 2022, ABFE). To our knowledge, this is the first work to  
058 demonstrate Boltz-2 as a superior oracle in practice for generative frameworks over the currently  
059 standard molecular docking. Second, we change the starting population in MOLLEO to consist of  
060 ligands from the large protein-ligand database BindingDB (Liu et al., 2007), focusing the algorithm  
061 toward the exploitation of existing strong binders. Third, we construct a semi-synthetic dataset  
062 based on BindingDB for improving the LLM’s lead optimization capabilities. We use this dataset to  
063 fine-tune a small LLM, and significantly improve the quality of its generated ligands.

064 To summarize, we present MOLLEO+, an optimized framework built upon the state-of-the-art  
065 MOLLEO (Wang et al., 2025), greatly improving its performance via the following contributions:

- 066
- 067 • We replace the docking-based fitness evaluator with Boltz-2 (Passaro et al., 2025) and show  
068 that it increases the mean Absolute Binding Free Energy of generated molecules by over  
069 100%.
- 070
- 071 • We utilize a starting population of ligands based on BindingDB, which increases mean  
072 predicted binding affinity of generated compounds by up to 15%.
- 073
- 074 • We develop a novel post-training framework to fine-tune LLMs for lead optimization tasks  
075 using a semi-synthetic dataset. We demonstrate its effectiveness by fine-tuning a small  
076 LLM and significantly improving the quality of its generated molecules.
- 077

## 078 2 RELATED WORK

### 079 2.1 MOLECULAR GENERATIVE MODELS

080

081 Most generative models for small-molecule drug design rely on an external oracle that approximates  
082 the binding strength of a ligand to a protein target. Graph-GA (Jensen, 2019) is an evolutionary  
083 algorithm that keeps track of an active population of molecules, for which their fitness is evalu-  
084 ated by some relevant oracle for the desired optimization property. It executes algorithmic random  
085 crossovers and mutations at particular rings and bonds within ligands of the active population, pro-  
086 gressively yielding molecules with more desirable properties as the algorithm progresses. Other  
087 frameworks have relied on machine learning methods to learn the implicit probability distribution of  
088 some input set, ideally generalizing to high performance in the full chemical space. Frameworks like  
089 TAGMol (Dorna et al., 2024) and DecomptOpt (Zhou et al., 2024) rely on conditional diffusion mod-  
090 els that are further guided toward strong generations by an oracle and some external optimization  
091 framework. Pocket2Mol (Peng et al., 2025) employs a graph neural network comprised of several  
092 encoder and predictor modules that auto-regressively predicts the location and type of each subse-  
093 quent ligand atom based on existing ligand atoms and the protein pocket. Notably, Pocket2Mol does  
094 not rely on any external oracle in its generation, only the inherent probability distribution learned  
095 during training.

096

097 Recently, there has been an understanding that common, cheap binding affinity oracles such as  
098 AutoDock (Trott & Olson, 2009) are inaccurate in predicting properties that reflect real-life experi-  
099 mental activity (Handa et al., 2023). Physics-based molecular dynamics simulations, e.g. Absolute  
100 Binding Free Energy (Feng et al., 2022, ABFE), are currently known to be the most accurate in  
101 binding affinity prediction, but they are extremely expensive to run and are thus unrealistic candi-  
102 dates for an oracle that may need to be called on tens of thousands of times within an optimization  
103 framework. MF-LAL (Eckmann et al., 2025) is an active learning framework that aims to remedy  
104 this problem through a multi-fidelity approach that balances feedback from expensive oracles (e.g.  
105 ABFE) and inexpensive oracles (e.g. AutoDock). This results in generations that are more optimal  
106 by assessment of the most accurate free energy methods. Ultimately, for the most real-life applicable  
107 results from generative models, these high-accuracy molecular dynamics predictors should be of the  
utmost consideration.

## 2.2 LLM-BASED APPROACHES

Previous work for incorporating LLMs in drug discovery has been relatively limited. There have been efforts in creating specialized models for drug discovery tasks. Models like Y-Mol (Ma et al., 2024) and DrugGen (Sheikholeslami et al., 2025) do this through a combination of pre-training and fine-tuning. However, these models are inherently designed to be one-shot at generation and property prediction, which does not comprise a full and rigorous optimization framework.

The current state-of-the-art in LLM generative frameworks is MOLLEO (Wang et al., 2025), which is a modification of the Graph-GA algorithm (Jensen, 2019). It utilizes LLMs to make structural modifications (crossovers and mutations) to the ligand population. This incorporation of LLMs into the algorithm resulted in strong results for protein-ligand optimization on 3 protein targets, demonstrating the potential of these inherently chemistry-aware large models to be a competitive generative framework in drug discovery. Due to the use of a natural language model as the operator, MOLLEO employs a string representation of small molecules, using both the Simplified Molecular Input Line Entry System (Weininger, 1988, SMILES) and Self-Referencing Embedded Strings (Krenn et al., 2020, SELFIES) for various LLMs. We focus on SMILES in this work.

While previous models mentioned above have succeeded in fine-tuning more chemistry-aware LLMs, the intended one-shot nature of their generations make them unsuitable for use in a multi-step optimization process such as MOLLEO. In contrast, fine-tuning framework we introduce in this work is optimized for conditioned generation, in which the LLM needs to generate a molecule based on provided information of previous members in the ligand population. In this way, our fine-tuning approach is more narrow and focused than previous work, meant for particular use within long optimization frameworks.

## 3 METHODOLOGY

**Problem Statement** Formally, we can represent our molecular optimization problem as

$$m^* = \operatorname{argmin}_{m \in M} \Phi_p(m)$$

where  $m$  is any valid molecule (ligand) and  $M$  is the entire valid chemical space.  $\Phi_p : M \rightarrow \mathbb{R}$  is an evaluation function that predicts the scalar binding free energy ( $\Delta G$ , in kcal/mol) of  $m$  to the protein binding target  $p$ . Lower binding free energy indicates stronger binding. We aim to find the optimal molecule  $m^*$ , which minimizes the evaluation function (also called the oracle).

MOLLEO is a genetic algorithm that uses an LLM to generate offspring based on modifications of ligands in the population. Each offspring is subsequently evaluated by the function  $\Phi_p$ . The molecules with the highest "fitness" according to  $\Phi_p$  are chosen for the next population. The LLM performs both crossover and mutation operations, only falling back on algorithmic modifications if the LLM fails to generate a valid molecule. We now discuss the 3 main contributions that comprise MOLLEO+, which are visually represented in Figure 1.

### 3.1 BOLTZ-2 AS A ORACLE

Boltz-2 (Passaro et al., 2025) is a new biomolecular foundation model that utilizes a transformer-based, SE(3) equivariant architecture to carry out 3D structure prediction, and subsequent binding affinity estimation on the predicted structure. The authors show that Boltz-2 approaches the accuracy of much more expensive gold-standard free energy methods like Absolute Binding Free Energy (ABFE) on their evaluation set, at around 1/1000 the cost. Notably, it is the first pure deep learning model to approach this kind of accuracy.

In this work, we replace the docking-based reward function used in MOLLEO with the more accurate affinity predictions from Boltz-2, which adds minimal computational cost. Formally, we change the original MOLLEO evaluation function  $\Phi_p$  from AutoDock to Boltz-2 for any protein target  $p$  with a known amino acid sequence. In other words, we directly utilize Boltz-2 affinity prediction to assign a fitness score to every generated ligand offspring. To our knowledge, this is the first work to demonstrate the advantages of using Boltz-2 as an oracle within a generative framework.

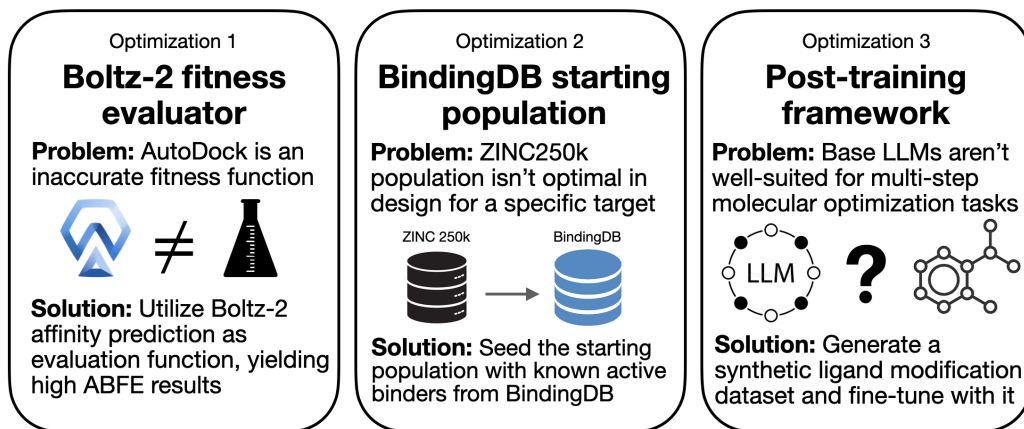


Figure 1: **The 3 primary optimizations that comprise MOLLEO+.** (1) We employ Boltz-2 as an oracle for improved ABFE results. (2) We utilize BindingDB to form a much stronger basis for optimization. (3) We propose a novel fine-tuning framework to steer LLMs toward stronger molecule generations.

### 3.2 OPTIMIZING STARTING POPULATION OF MOLLEO

The strength and diversity of the starting population for a genetic algorithm is crucial for the quality of generated compounds, because all ligand offspring are derived in some way from the structures present in the starting population. The original MOLLEO algorithm uses a random sample of ZINC 250k (Sterling & Irwin, 2015) compounds as the initial population. Although this data set does provide a diverse pool of structures to build on, the molecules present are inherently not designed for any particular target.

Our optimization to MOLLEO involves employing the large protein-ligand database BindingDB (Liu et al., 2007) instead of ZINC 250k to give the MOLLEO algorithm a significantly stronger starting point. With BindingDB, we are able to selectively pick strong known binders to the particular target that we are interested in, comprising an initial population that immediately promises much greater experimental activity. This focuses the algorithm more on the exploitation of existing strong binders (which are often known during drug discovery projects), rather than exploration based on non target-specific molecular structures.

To form this starting pool, we first separate the set of BindingDB ligands corresponding to the protein target we want to target into clusters using the Butina algorithm, which creates clusters based on the pairwise Tanimoto similarity of all ligands to each other. We use a distance threshold of 0.4. This ensures that ligands are structurally diverse across different clusters, because very similar ligands are all grouped within the same clusters. This is desirable because we want the algorithm to have access to a diverse set of structures and molecules, giving it the potential to create entirely novel molecules through combinations and crossovers. From there, we sampled the ligand with the best binding affinity from each cluster, forming a set of strong-binding, structurally diverse ligands. After sorting this list of ligands, we provide the top  $n$  ligands with the best binding affinity as the starting population for MOLLEO. Analysis of the diversity of the BindingDB starting population in comparison to the ZINC 250k starting population can be found in Appendix B

### 3.3 FINE-TUNING WITH BINDINGDB

We propose a fine-tuning strategy to imbue domain knowledge and specifically enable an LLM to perform better at each optimization step of the MOLLEO process, i.e. every time the LLM makes a crossover/mutation based on previous ligands. We can formulate the process of each individual optimization step  $i$  as  $m_i = LLM(h_{<i})$  where  $h_{<i}$  is the prior information (SMILES and binding affinity) given about previous ligands in the population, and  $m_i$  is the newly generated molecule. We want to tune an LLM that can most effectively process  $h_{<i}$  to yield  $m_i$  that minimizes the binding affinity evaluation function  $\Phi_p$ . To achieve this, we propose a supervised fine-tuning (SFT)

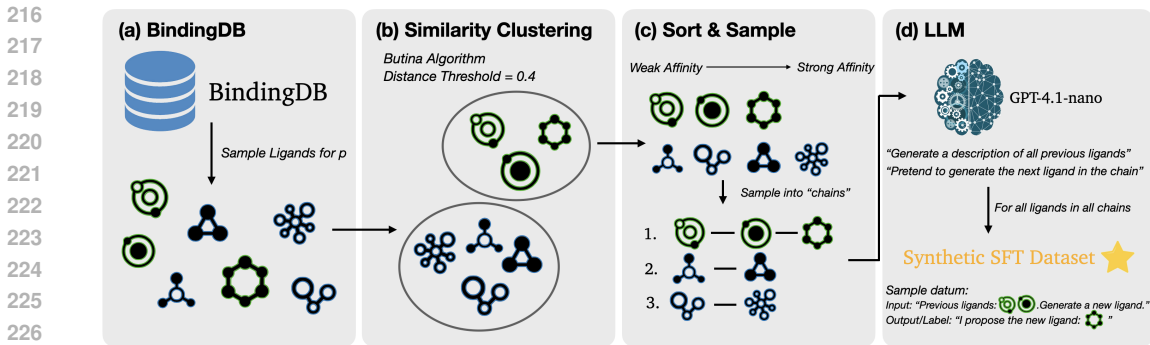


Figure 2: **Pipeline for preparing SFT dataset.** (a) We sample ligands for the desired protein target  $p$  from BindingDB. (b) We cluster the ligands by the Butina algorithm. (c) We sort the ligands by binding affinity within each cluster, then sample them into several chains. (d) We utilize a LLM to generate our semi-synthetic dataset from the ligand chains.

framework for any particular protein target  $p$ , involving the creation of a semi-synthetic dataset followed by subsequent usage of the dataset in SFT.

To form a semi-synthetic dataset for supervised fine-tuning using BindingDB, we begin in a similar way to the clustering method described above for the formation of the BindingDB starting population. We form  $n$  distinct clusters from the ligand pool for our desired protein target, using Butina clustering with distance threshold 0.4. Then within each cluster, we first sort the ligands by affinity, then form a series of "ligand chains". This is done by first picking a weak affinity ligand, then repeatedly selecting a ligand with binding affinity strictly stronger than the current. The result is that for each cluster, we end up with several chains of ligands that are ordered with increasing binding affinity. All ligands within a chain are guaranteed to be relatively similar in structure due to the clustering. The goal of this approach is to form a dataset where an LLM learns to make decisions that change a weak-binding ligand into a guaranteed strong-binding one as it moves down the chain during training. The changes are usually minimal due to the structural similarity, so each chain represents a somewhat realistic series of modifications that a medicinal chemist might make. An example of one of these ligand chains generated for the c-MET target can be found in Appendix C.1.

Employing the ligand chains, we generate a semi-synthetic text dataset using an LLM. We employ GPT 4.1 nano (OpenAI et al., 2024) for cost efficiency. For each ligand chain, we have the LLM generate an artificial input and output response that mimics how we want our tuned LLM to generate a molecule based on previous molecules. Formally, for any ligand in position  $i$  of a chain, we create our prior information  $h_{0..i}$  by utilizing the LLM to summarize the information from all previous ligands in positions 0 to  $i$ . Since we want our tuned model to generate the ligand at position  $i$ , we utilize the LLM to generate a sample output that includes ligand  $i$  as the final generation. Then a full input/output datum for the dataset is comprised of the prior  $h_{0..i}$  as the input and a sample output that includes the desired molecule  $m_i$ . Fine-tuning an LLM on this dataset guides the LLM to generate the strong molecule  $m_i$  given prior information  $h_{0..i}$ , which is what we want the model to do within a long optimization process such as MOLLEO. The exact details and prompts for how we utilize the ligand chains to form an SFT dataset can be found in Appendix C.2. This entire process is visually demonstrated in Figure 2.

This semi-synthetic dataset is used in a classic supervised fine-tuning run. We employ a train-validation split on the dataset, and progress until we observe the validation loss reach a plateau. We apply this training framework to the relatively small Llama-3.1-8B-Instruct model (Grattafiori et al., 2024). Details about the SFT training process are provided in Appendix C.3

## 4 RESULTS

### 4.1 IMPROVING ABFE WITH BOLTZ-2 ORACLE

We first evaluate the impact of using Boltz-2 as an oracle instead of AutoDock. Table 1 compares the mean Absolute Binding Free Energy (ABFE) scores (Feng et al., 2022) of ligands generated for the c-MET protein target using Boltz-2 (Passaro et al., 2025) and AutoDock docking (Trott & Olson, 2009) as the fitness evaluator for MOLLEO. We also report the 1st, 2nd, and 3rd strongest molecules generated by these methods. Our setup for ABFE calculations is provided in Appendix A. We also benchmark against molecules generated by MF-LAL (Eckmann et al., 2025), a VAE-based generative method that focuses on achieving strong ABFE results using a multi-fidelity approach.

Table 1: c-MET ABFE results (kcal/mol) for Autodock, Boltz-2, and MF-LAL

Method	Count	Mean $\pm$ SD	1st	2nd	3rd
MF-LAL	10	-4.3 $\pm$ 3.7	-8.7	-8.5	-8.3
MOLLEO (AutoDock)	20	-3.8 $\pm$ 4.2	-12.8	-8.8	-8.7
MOLLEO (Boltz-2)	20	<b>-8.7 <math>\pm</math> 4.6</b>	<b>-15.64</b>	<b>-14.04</b>	<b>-13.98</b>

For these calculations, we take the top 20 best molecules generated from each run according to the respective oracle. We can see that MOLLEO does not beat the MF-LAL baseline in terms of mean affinity, but simply incorporating Boltz-2 as the evaluation function improves the results drastically. MOLLEO with Boltz-2 results in compounds with much better ABFE scores than with AutoDock, having a difference in mean ABFE score of -4.8 kcal/mol, a percentage increase of over 100%. MOLLEO with Boltz-2 yields  $p = 0.0007$  from the one-sided independent Student’s t-test against MOLLEO with AutoDock, and  $p = 0.007$  against MF-LAL. Note that these runs are done on the base MOLLEO setup, without the BindingDB starting population described previously.

Given the demonstrated advantages of using Boltz-2 within a generative framework, we are motivated to provide further general analysis of the correlation between Boltz-2, AutoDock, and ABFE. In Figure 3, we take 32 compounds for c-MET, 16 of which are known binders, and 16 of which are presumed inactive binders. We calculate the ABFE, Boltz-2, and AutoDock binding affinities for all 32 compounds. We exclude results for any failed AutoDock or Boltz-2 runs.

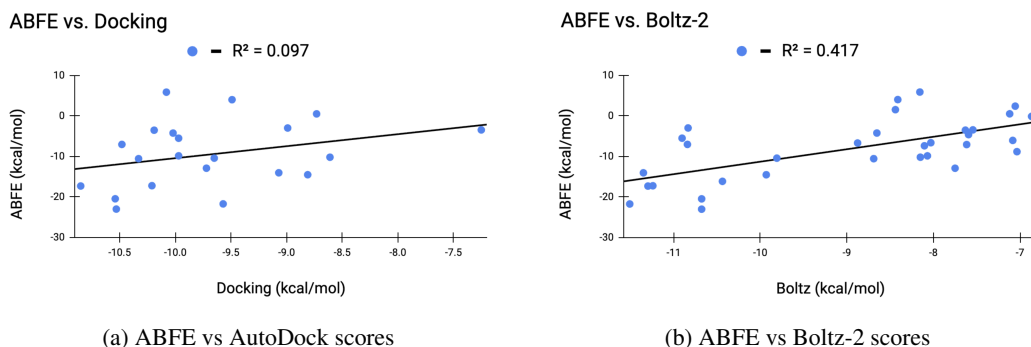


Figure 3: Comparison of correlation between AutoDock & ABFE and Boltz-2 & ABFE for 32 known compounds for the c-MET protein target. We observe a significantly higher correlation between Boltz-2 and ABFE as compared to AutoDock.

We see that ABFE and AutoDock docking show  $r^2 = 0.09$  among the 32 compounds, while ABFE and Boltz-2 show  $r^2 = 0.42$ . As an oracle nearly 1000x less computationally expensive than ABFE, Boltz-2 shows exceptional correlation with ABFE, especially in comparison to docking. Furthermore, we calculate the ROC-AUC score for Boltz-2 and docking, to see how well they can separate binders from non-binders. Boltz-2 scores 0.95 for this metric, while AutoDock scores 0.84. Due

to computational and time constraints regarding expensive ABFE calculations, we are only able to provide results for the c-MET target at this time.

Thus, we demonstrate that not only does Boltz-2 have stronger correlation with the most accurate gold-standard computational methods, but that it also has practical application within a generative framework, acting as a more accurate evaluator that guides generated compounds towards higher ABFE scores. We generally observe Boltz-2 to be approximately a factor of 10 more expensive to run than AutoDock; however, this difference is entirely negligible in comparison to the cost of molecular dynamics methods such as ABFE.

#### 4.2 IMPROVED BINDING AFFINITY WITH MOLLEO+

Next, we demonstrate the performance of MOLLEO+ on two protein targets, c-MET and BRD4. Structurally speaking, these targets are quite dissimilar, making our results more robust when considering both targets. Every MOLLEO run terminates at 1000 oracle calls, with an initial population (and population size) of 120 and offspring size of 70. We report all results with Boltz-2 calculated binding affinities instead of ABFE due to computational constraints, but rely on the strong results shown in the previous section to support the validity of *relative* differences between methods.

Table 2 shows the comparison of binding affinity measured by Boltz-2 across different methods. We compare with the base MOLLEO algorithm, as well as with two additional baselines: MF-LAL and Pocket2Mol (Peng et al., 2025). Both models have previously been observed to yield molecules with high ABFE scores (Eckmann et al., 2025).

We report 4 metrics:

1. Mean and standard deviation in binding affinity (kcal/mol), as predicted by Boltz-2.
2. Number of ligands that exceed a strong-binding threshold of -11 kcal/mol.
3. Quantitative estimate of drug-likeness (Bickerton et al., 2012, QED), a scale from 0-1 for which higher QED indicates higher drug-likeness.
4. Synthetic accessibility (Ertl & Schuffenhauer, 2009, SA), a scale from 1-10 for which lower SA indicates greater ease of molecular synthesis.

Table 2: Boltz-2 affinity (kcal/mol), QED, and SA for baselines and MOLLEO+

Method	c-MET				BRD4			
	Mean $\pm$ SD	# Strong	QED	SA	Mean $\pm$ SD	# Strong	QED	SA
MF-LAL	-7.4 $\pm$ 1.2	0	<b>0.56</b>	<b>3.7</b>	-8.8 $\pm$ 1.2	0	<b>0.57</b>	3.7
Pocket2Mol	-11.2 $\pm$ 0.3	7	0.38	4.7	-10.2 $\pm$ 0.5	1	0.36	4.5
MOLLEO	-9.0 $\pm$ 0.4	0	0.17	4.0	-8.5 $\pm$ 0.6	0	0.19	4.5
MOLLEO (BindingDB)	-10.2 $\pm$ 0.5	4	0.20	3.8	-9.2 $\pm$ 0.3	0	0.12	4.2
MOLLEO (Boltz-2)	-11.2 $\pm$ 0.1	9	0.18	4.8	-10.7 $\pm$ 0.1	2	0.12	4.9
MOLLEO+ (ours)	<b>-11.9 <math>\pm</math> 0.1</b>	<b>10</b>	0.20	4.5	<b>-11.9 <math>\pm</math> 0.2</b>	<b>10</b>	0.36	3.5
MOLLEO+ (Llama)	-10.9 $\pm$ 0.1	4	0.39	4.0	-10.7 $\pm$ 0.1	2	0.43	3.8
MOLLEO+ (Llama FT)	<u>-11.6 <math>\pm</math> 0.1</u>	<b>10</b>	0.35	<b>3.7</b>	<u>-11.4 <math>\pm</math> 0.1</u>	<b>10</b>	0.45	<b>3.3</b>

MOLLEO is the original, unmodified algorithm. MOLLEO (BindingDB) is the result of utilizing the BindingDB starting population while keeping AutoDock as the oracle. MOLLEO (Boltz-2) is the result of changing the oracle to Boltz-2 instead of AutoDock while keeping the original ZINC 250K starting population. MOLLEO+ is our full method, the result of combining both the Boltz-2 and the BindingDB starting population optimizations. All MOLLEO runs are done with GPT-4.1-mini for cost efficiency, as opposed to GPT-4 used in the original MOLLEO paper. At the bottom, we give the results of using the Llama-3.1-8B-Instruct model within MOLLEO, as well as with our fine-tuned version of this model. For each result, we run the same method 3 times with different randomization seeds for greater rigor.

All metrics are reported for a sample of generated ligands. We first Butina cluster the full pool of generated molecules (with similarity threshold = 0.6), then take the best 10 scores that belong to

distinct clusters. This way, we more effectively assess the quality of structurally unique generations. Additionally, to focus solely on the LLM performance, we remove compounds from MOLLEO runs generated by the default crossover/mutation operators, which the algorithm falls back on if the LLM generates an invalid molecule.

In terms of mean affinity, we see that the original MOLLEO algorithm does not significantly outperform the non-MOLLEO baselines on either target. However, we observe a substantial increase in affinity both when we utilize the BindingDB starting population ( $p = 0.03$  against the original MOLLEO for c-MET,  $p = 0.12$  for BRD4) and when we use Boltz-2 as the oracle ( $p < 0.001$  against the original MOLLEO for both targets) independently of each other. Furthermore, MOLLEO+ yields another significant increase in mean affinity over either previous method by itself, with the combination of both BindingDB and Boltz-2 having significant effects on the affinity results. ( $p < 0.001$  against MOLLEO with Boltz-2 for both targets). We also observe a significant increase in affinity between our fine-tuned small Llama model and the untuned version ( $p < 0.001$  for both targets). We further measure the number of diverse, top compounds that exceed an activity threshold of -11 kcal/mol; we see that incorporating BindingDB in the starting population increases this metric significantly, as does the fine-tuning process for the Llama model.

We observe that, in general, QED metrics are weaker in MOLLEO+ runs than within the baselines (although, notably, we observe strong results with our fine-tuned Llama model). We note that the original MOLLEO had a similar issue in this area, showing similar if not even weaker QED and SA results compared to MOLLEO+. As an evolutionary algorithm, MOLLEO can support multi-objective optimization through Pareto front optimization. We did not explore multi-objective optimization in this work as our focus was on protein-ligand binding affinity and translation to real-world experimental activity; however, as MOLLEO+ does not suffer any observed decrease in other desirable metrics such as QED and SA as compared to MOLLEO, we expect to still see strong results in other properties through application of the multi-objective framework to our method. In other words, we observe a clear increase in binding affinity in MOLLEO+ with no decrease in desirable ligand-specific properties, implying an unconditional improvement over the original algorithm and a preserved potential for strong performance in multi-objective optimization. We aim to explore this concretely in future work.

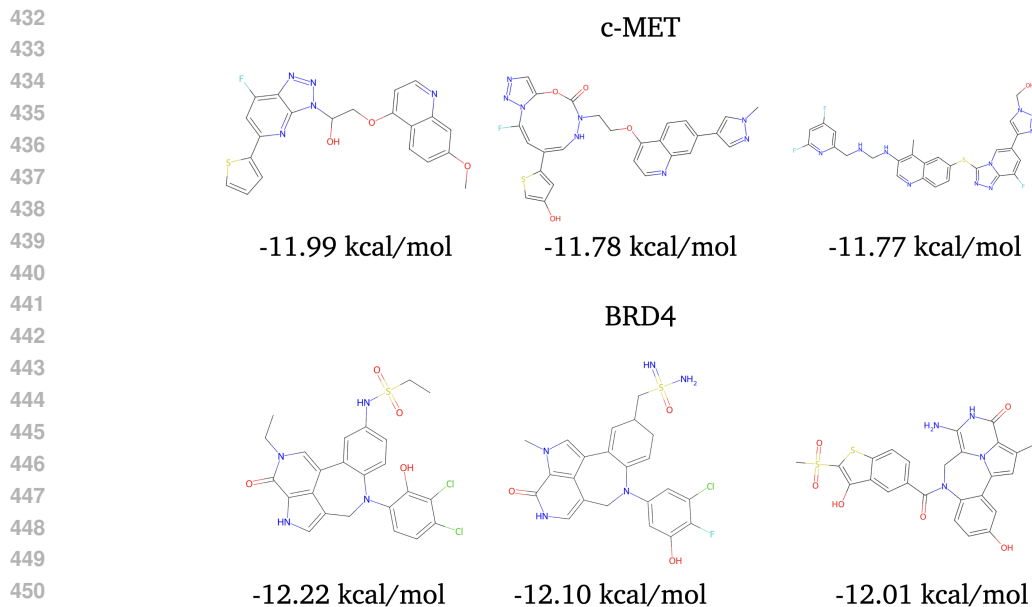
#### 4.3 ANALYSIS OF SIMILARITY AND NOVELTY

A significant part of the molecular generation process is producing molecules that are both strong binders and relatively novel in structure. We analyze the effectiveness of MOLLEO+ in this area by applying a filter to the results, only considering generated ligands with Tanimoto similarity  $< 0.5$  to *any* ligand in the starting population. The results of applying this filter are shown in Table 3. We provide the average maximum similarity to any ligand in the starting population for generated ligands, then measure the mean of the top 10 diverse ligands with this filter applied.

Table 3: Comparison of average maximum similarity and filtered mean affinity (kcal/mol)

Method	c-MET		BRD4	
	Avg. Max Sim.	Filtered Mean $\pm$ SD	Avg. Max Sim.	Filtered Mean $\pm$ SD
MOLLEO	<b>0.33</b>	-9.0 $\pm$ 0.4	<b>0.32</b>	-8.5 $\pm$ 0.6
MOLLEO (Boltz-2)	0.34	-11.2 $\pm$ 0.1	<b>0.32</b>	-10.7 $\pm$ 0.1
MOLLEO+ (ours)	0.39	<b>-11.7 <math>\pm</math> 0.1</b>	0.40	<b>-11.5 <math>\pm</math> 0.3</b>
MOLLEO+ (Llama)	0.36	-10.2 $\pm$ 0.6	0.44	-8.7 $\pm$ 0.7
MOLLEO+ (Llama FT)	0.44	<u>-11.2 <math>\pm</math> 0.3</u>	0.37	<u>-11.0 <math>\pm</math> 0.2</u>

We observe that MOLLEO+ generally suffers from slightly lower novelty within its generated pool of molecules. This is a consequence of utilizing strong structures in BindingDB as the starting population. Because the provided initial structures are already very strong, the strongest generated ligands are likely to be close derivatives of those initial structures. Then as the evolutionary algorithm progresses, it selects for the strongest ligands, resulting in higher similarity throughout the population. In contrast, the starting structures in ZINC 250K are not guaranteed to be strong for any particular protein target, so for novel generated ligands to be strong, they necessarily have to be



452 Figure 4: Visualizations of top 3 ligands for c-MET and BRD4 generated by MOLLEO+ with  $< 0.5$   
453 Tanimoto similarity to any ligand in the starting population and  $< 0.6$  similarity to each other.  
454

455 dissimilar to much of the starting population. Because of this, we observe higher similarity on average  
456 in MOLLEO+. However, the filtered mean shows us that even with a less novel ligand pool *on*  
457 *average*, the novel generations of MOLLEO+ with BindingDB are still significantly stronger than  
458 the novel generations of MOLLEO with ZINC 250K ( $p = 0.01$  against the Boltz-2 run for c-MET,  
459  $p = 0.03$  for BRD4). Visualizations of the top ligands for c-MET and BRD4 when applying the  
460 similarity filter are shown in Figure 4.  
461

462 For extended rigor, we further test filters using more constraining Tanimoto similarity thresholds of  
463 0.45 and 0.4. Additionally, we test a filter based on scaffold-level similarity (at similarity thresh-  
464 old 0.5) by evaluating the similarity in the Murcko Scaffolds generated by ligands instead of full-  
465 molecule Tanimoto similarity. Mean affinity for all three of these filters are shown in Table 4 on  
466 MOLLEO (Boltz-2) and MOLLEO+ results, for which the comparison between the two is most  
467 pertinent to further rigor, since we are most interested in how introducing BindingDB in particular  
468 impacts generation diversity. We report the filtered binding affinity means as well as the independ-  
469 ent Student’s t-test p-values for the alternative hypothesis: MOLLEO+ mean affinity  $<$  MOLLEO  
(Boltz-2) mean affinity.  
470

471 Table 4: Affinity results after applying 3 separate filters: similarity threshold = 0.45, similarity  
472 threshold = 0.4, and Murcko scaffold similarity (with threshold = 0.5)  
473

Method	c-MET (Mean Affinity)			BRD4 (Mean Affinity)		
	Sim = 0.45	Sim = 0.4	Scaffold-level Sim.	Sim = 0.45	Sim = 0.4	Scaffold-level Sim.
MOLLEO (Boltz-2)	-11.2 $\pm$ 0.1	-11.2 $\pm$ 0.1	-11.2 $\pm$ 0.1	-10.7 $\pm$ 0.1	-10.7 $\pm$ 0.1	-10.7 $\pm$ 0.1
MOLLEO+ (ours)	<b>-11.6</b> $\pm$ 0.1	<b>-11.3</b> $\pm$ 0.1	<b>-11.6</b> $\pm$ 0.1	<b>-11.3</b> $\pm$ 0.2	<b>-11.0</b> $\pm$ 0.1	<b>-11.3</b> $\pm$ 0.1
T-test P-value	$< 0.01$	0.08	0.02	0.04	0.06	$< 0.01$

480 We observe that, under these additional filters, the incorporation of BindingDB still yields stronger  
481 molecules constrained to the necessity for structural diversity. This is true even when evaluating  
482 more fine-grained scaffold-level similarity. However, at similarity thresholds lower than 0.4, the  
483 gain in affinity from introducing BindingDB becomes minimal. Due to this, we acknowledge that  
484 the overall diversity of strong results from MOLLEO+ is generally weaker than when that of using  
485 a ZINC 250K starting population. However, given that our primary motivation for this work is to  
create a framework that takes advantage of known information to create molecules suitable for real-

486 world drug discovery, we do not consider this an imminently crucial problem. Although the highest  
487 possible generation diversity is certainly desirable, we believe that the demonstrated gains in affinity  
488 through several levels of restrictive similarity filters show that MOLLEO+ performs well enough  
489 in novelty to support its improvement over MOLLEO as a tool to assist drug-discovery pipelines,  
490 particularly for lead-optimization tasks where we have prior information and novelty is not of utmost  
491 importance. In other words, we believe that we currently demonstrate strong-enough results in  
492 this section to justify the larger intended use-case for our framework, which involves generation of  
493 strong, relatively novel real-world candidate molecules that are optimized for high scores on the  
494 most accurate free-energy benchmarks. We plan to utilize multi-objective optimization to further  
495 strengthen novelty results in future work.

## 497 5 DISCUSSION & CONCLUSION

499 We present MOLLEO+, an optimization of the MOLLEO framework that demonstrably improves  
500 the design of LLM-based protein-ligand drugs. We show that Boltz-2 is a better fitness function  
501 than docking, producing compounds that are more likely to show real-world binding. This result  
502 is notable given previous concerns that Boltz-2 performs poorly out-of-distribution, and suggests  
503 that Boltz-2, instead of docking, should be used as an oracle for other molecular generative models.  
504 We also modify the starting population of MOLLEO, resulting in significantly stronger generated  
505 structures and molecules throughout the algorithm. Finally, we present a fine-tuning framework  
506 that employs BindingDB to create a novel semi-synthetic dataset, which improves the molecular  
507 generation abilities of a small Llama 3 model.

508 We demonstrate significant advantages of the MOLLEO+ framework in generating molecules with  
509 high Boltz-2 scores. Due to the demonstrated increase in ABFE and the additional correlation  
510 analysis between ABFE and Boltz-2, we are confident that this increase in Boltz-2 affinity over  
511 MOLLEO is somewhat correlative to an increase in ABFE. Through this, we are comfortable with  
512 claiming that MOLLEO+ is a significantly more effective framework for producing molecules that  
513 may show real-world experimental activity.

514 Our fine-tuning method also shows great promise in improving the generation quality of small  
515 molecules through post-training alone. We observe not only a significant increase in binding affinity,  
516 but also great success in QED and SA. While we acknowledge that we do not yet exceed the state-of-  
517 the-art (GPT-4) in terms of binding affinity with our very small fine-tuned model, we demonstrate  
518 extremely strong relative improvements, and hypothesize that the same post-training method can  
519 be applied to larger models and yield a similar relative increase in performance. We leave this for  
520 exploration in future work. We did have some specific concerns about whether this fine-tuning pro-  
521 cess actually improved the *quality* of generated molecules, or simply molded the model to obey  
522 the MOLLEO answer format. We observed that the untuned model fails to follow the answer for-  
523 mat for a significant portion of its generations, leading to failed parsing and thus an unconsidered,  
524 potentially-valid generated molecule. We ablate this potential flaw in Appendix C.4.

525 **Limitations** While our BindingDB approach to MOLLEO demonstrably improves the perfor-  
526 mance on the c-MET and BRD4 targets, we recognize that these are both very well-studied targets.  
527 For less studied protein targets, this method may be entirely inapplicable if there are not enough  
528 *diverse* known binders to comprise a starting population. This also somewhat applies to our fine-  
529 tuning framework; however, we demonstrate in Appendix D that we can utilize other ligands from  
530 BindingDB and still achieve comparable performance.

531 **Ethics Statement** We recognize that improved molecular optimization frameworks may be uti-  
532 lized to generate chemically dangerous compounds. However, since our work does not consider  
533 complicated properties and requirements for generation and synthesis of harmful compounds, our  
534 contribution is not imminently problematic in this direction.

536 **Reproducibility Statement** We provide all details of our work and implementation in the Method-  
537 ology section, as well as in sections of the Appendix. We disclose our parameters for ABFE, our  
538 parameters for fine-tuning, and all details needed to reproduce our experiments. Additionally, we  
539 attach all of our relevant code as supplementary material in this submission, which is documented  
with instructions on how to run everything and reproduce our results.

540 **LLM Usage** While our methodology focuses on the use of LLMs as a scientific tool, we did not  
541 employ any LLMs in either the ideation or composition of this work. All text in this work were  
542 written solely by the authors, as are all figures, tables, and data. We do not employ any LLM  
543 assistance in the writing process, and all written text is our own.

## 544 REFERENCES

- 545  
546  
547 Stephen F. Altschul, Warren Gish, Webb Miller, Eugene W. Myers, and David J. Lipman. Basic  
548 local alignment search tool. *Journal of Molecular Biology*, 215(3):403–410, October 1990. ISSN  
549 0022-2836. doi: 10.1016/s0022-2836(05)80360-2. URL [http://dx.doi.org/10.1016/  
550 S0022-2836\(05\)80360-2](http://dx.doi.org/10.1016/S0022-2836(05)80360-2).
- 551 G. Richard Bickerton, Gaia V. Paolini, Jérémy Besnard, Sorel Muresan, and Andrew L. Hopkins.  
552 Quantifying the chemical beauty of drugs. *Nature Chemistry*, 4(2):90–98, January 2012. ISSN  
553 1755-4349. doi: 10.1038/nchem.1243. URL [http://dx.doi.org/10.1038/nchem.  
554 1243](http://dx.doi.org/10.1038/nchem.1243).
- 555 Vineeth Dorna, D. Subhalingam, Keshav Kolluru, Shreshth Tuli, Mrityunjay Singh, Saurabh Sing-  
556 gal, N. M. Anoop Krishnan, and Sayan Ranu. Tagmol: Target-aware gradient-guided molecule  
557 generation, 2024. URL <https://arxiv.org/abs/2406.01650>.
- 558  
559 Peter Eckmann, Kunyang Sun, Bo Zhao, Mudong Feng, Michael K. Gilson, and Rose Yu. Limo:  
560 Latent inceptionism for targeted molecule generation, 2022. URL [https://arxiv.org/  
561 abs/2206.09010](https://arxiv.org/abs/2206.09010).
- 562 Peter Eckmann, Dongxia Wu, Germano Heinzelmann, Michael K. Gilson, and Rose Yu. Mf-lal:  
563 Drug compound generation using multi-fidelity latent space active learning, 2025. URL [https://  
564 arxiv.org/abs/2410.11226](https://arxiv.org/abs/2410.11226).
- 565  
566 Peter Ertl and Ansgar Schuffenhauer. Estimation of synthetic accessibility score of drug-like  
567 molecules based on molecular complexity and fragment contributions. *Journal of Chemin-  
568 formatics*, 1(1), June 2009. ISSN 1758-2946. doi: 10.1186/1758-2946-1-8. URL [http://  
569 dx.doi.org/10.1186/1758-2946-1-8](http://dx.doi.org/10.1186/1758-2946-1-8).
- 570 Mudong Feng, Germano Heinzelmann, and Michael K. Gilson. Absolute binding free energy  
571 calculations improve enrichment of actives in virtual compound screening. *Scientific Reports*,  
572 12(1), August 2022. ISSN 2045-2322. doi: 10.1038/s41598-022-17480-w. URL [http://  
573 dx.doi.org/10.1038/s41598-022-17480-w](http://dx.doi.org/10.1038/s41598-022-17480-w).
- 574  
575 Tianfan Fu, Wenhao Gao, Connor W. Coley, and Jimeng Sun. Reinforced genetic algorithm for  
576 structure-based drug design, 2022. URL <https://arxiv.org/abs/2211.16508>.
- 577  
578 Aaron Grattafiori, Abhimanyu Dubey, Abhinav Jauhri, Abhinav Pandey, Abhishek Kadian, et al.  
579 The llama 3 herd of models, 2024. URL <https://arxiv.org/abs/2407.21783>.
- 580 Koichi Handa, Morgan C. Thomas, Michiharu Kageyama, Takeshi Iijima, and Andreas Ben-  
581 der. On the difficulty of validating molecular generative models realistically: a case study  
582 on public and proprietary data. *Journal of Cheminformatics*, 15(1), November 2023. ISSN  
583 1758-2946. doi: 10.1186/s13321-023-00781-1. URL [http://dx.doi.org/10.1186/  
584 s13321-023-00781-1](http://dx.doi.org/10.1186/s13321-023-00781-1).
- 585 Germano Heinzelmann and Michael K. Gilson. Automation of absolute protein-ligand binding free  
586 energy calculations for docking refinement and compound evaluation. *Scientific Reports*, 11(1),  
587 January 2021. ISSN 2045-2322. doi: 10.1038/s41598-020-80769-1. URL [http://dx.doi.  
588 org/10.1038/s41598-020-80769-1](http://dx.doi.org/10.1038/s41598-020-80769-1).
- 589 Emiel Hoogeboom, Victor Garcia Satorras, Clément Vignac, and Max Welling. Equivariant diffu-  
590 sion for molecule generation in 3d, 2022. URL <https://arxiv.org/abs/2203.17003>.
- 591  
592 Edward J. Hu, Yelong Shen, Phillip Wallis, Zeyuan Allen-Zhu, Yuanzhi Li, Shean Wang, Lu Wang,  
593 and Weizhu Chen. Lora: Low-rank adaptation of large language models, 2021. URL [https://  
arxiv.org/abs/2106.09685](https://arxiv.org/abs/2106.09685).

- 594 Jan H. Jensen. A graph-based genetic algorithm and generative model/monte carlo tree search for  
595 the exploration of chemical space. *Chemical Science*, 10(12):3567–3572, 2019. ISSN 2041-6539.  
596 doi: 10.1039/c8sc05372c. URL <http://dx.doi.org/10.1039/C8SC05372C>.  
597
- 598 Woosung Jeon and Dongsup Kim. Autonomous molecule generation using reinforcement  
599 learning and docking to develop potential novel inhibitors. *Scientific Reports*, 10(1):  
600 22104, 2020. doi: 10.1038/s41598-020-78537-2. URL [https://doi.org/10.1038/  
601 s41598-020-78537-2](https://doi.org/10.1038/s41598-020-78537-2).
- 602 Mario Krenn, Florian Häse, Akshat Kumar Nigam, Pascal Friederich, and Alan Aspuru-Guzik. Self-  
603 referencing embedded strings (SELFIES): A 100% robust molecular string representation. *Ma-  
604 chine Learning: Science and Technology*, 1(4):045024, October 2020. ISSN 2632-2153. doi: 10.  
605 1088/2632-2153/aba947. URL <http://dx.doi.org/10.1088/2632-2153/aba947>.  
606
- 607 Seul Lee, Jaehyeong Jo, and Sung Ju Hwang. Exploring chemical space with score-based out-of-  
608 distribution generation, 2023. URL <https://arxiv.org/abs/2206.07632>.
- 609 T. Liu, Y. Lin, X. Wen, R. N. Jorissen, and M. K. Gilson. Bindingdb: a web-accessible database  
610 of experimentally determined protein-ligand binding affinities. *Nucleic Acids Research*, 35  
611 (Database):D198–D201, January 2007. ISSN 1362-4962. doi: 10.1093/nar/gk1999. URL  
612 <http://dx.doi.org/10.1093/nar/gk1999>.
- 613 Tengfei Ma, Xuan Lin, Tianle Li, Chaoyi Li, Long Chen, Peng Zhou, Xibao Cai, Xinyu Yang, Dao-  
614 jian Zeng, Dongsheng Cao, and Xiangxiang Zeng. Y-mol: A multiscale biomedical knowledge-  
615 guided large language model for drug development, 2024. URL [https://arxiv.org/abs/  
616 2410.11550](https://arxiv.org/abs/2410.11550).
- 617
- 618 Eyal Mazuz, Guy Shtar, Bracha Shapira, and Lior Rokach. Molecule generation using transform-  
619 ers and policy gradient reinforcement learning. *Scientific Reports*, 13(1), May 2023. ISSN  
620 2045-2322. doi: 10.1038/s41598-023-35648-w. URL [http://dx.doi.org/10.1038/  
621 s41598-023-35648-w](http://dx.doi.org/10.1038/s41598-023-35648-w).
- 622 Juhwan Noh, Dae-Woong Jeong, Kiyoun Kim, Sehui Han, Moontae Lee, Honglak Lee, and  
623 Yousung Jung. Path-aware and structure-preserving generation of synthetically accessible  
624 molecules. In Kamalika Chaudhuri, Stefanie Jegelka, Le Song, Csaba Szepesvari, Gang Niu,  
625 and Sivan Sabato (eds.), *Proceedings of the 39th International Conference on Machine Learning*,  
626 volume 162 of *Proceedings of Machine Learning Research*, pp. 16952–16968. PMLR, 17–23 Jul  
627 2022. URL <https://proceedings.mlr.press/v162/noh22a.html>.
- 628
- 629 OpenAI, Josh Achiam, Steven Adler, Sandhini Agarwal, Lama Ahmad, et al. Gpt-4 technical report,  
630 2024. URL <https://arxiv.org/abs/2303.08774>.
- 631 Saro Passaro, Gabriele Corso, Jeremy Wohlwend, Mateo Reveiz, Stephan Thaler, Vignesh Ram  
632 Somnath, Noah Getz, Tally Portnoi, Julien Roy, Hannes Stark, David Kwabi-Addo, Dominique  
633 Beaini, Tommi Jaakkola, and Regina Barzilay. Boltz-2: Towards accurate and efficient binding  
634 affinity prediction. June 2025. doi: 10.1101/2025.06.14.659707. URL [http://dx.doi.  
635 org/10.1101/2025.06.14.659707](http://dx.doi.org/10.1101/2025.06.14.659707).
- 636 Xingang Peng, Shitong Luo, Jiaqi Guan, Qi Xie, Jian Peng, and Jianzhu Ma. Pocket2mol: Efficient  
637 molecular sampling based on 3d protein pockets, 2025. URL [https://arxiv.org/abs/  
638 2205.07249](https://arxiv.org/abs/2205.07249).
- 639
- 640 Eric F. Pettersen, Thomas D. Goddard, Conrad C. Huang, Elaine C. Meng, Gregory S. Couch,  
641 Tristan I. Croll, John H. Morris, and Thomas E. Ferrin. jscp;ucsf chimerax;scpi: Structure  
642 visualization for researchers, educators, and developers. *Protein Science*, 30(1):70–82, October  
643 2020. ISSN 1469-896X. doi: 10.1002/pro.3943. URL [http://dx.doi.org/10.1002/  
644 pro.3943](http://dx.doi.org/10.1002/pro.3943).
- 645 Mahsa Sheikholeslami, Navid Mazrouei, Yousof Gheisari, Afshin Fasihi, Matin Irajpour, and Ali  
646 Motaharynia. Druggen enhances drug discovery with large language models and reinforcement  
647 learning. *Scientific Reports*, 15(1), 2025. ISSN 2045-2322. doi: 10.1038/s41598-025-98629-1.  
URL <http://dx.doi.org/10.1038/s41598-025-98629-1>.

- 648 Teague Sterling and John J. Irwin. Zinc 15 – ligand discovery for everyone. *Journal of Chemical*  
649 *Information and Modeling*, 55(11):2324–2337, November 2015. ISSN 1549-960X. doi: 10.1021/  
650 acs.jcim.5b00559. URL <http://dx.doi.org/10.1021/acs.jcim.5b00559>.  
651
- 652 Oleg Trott and Arthur J. Olson. Autodock vina: Improving the speed and accuracy of docking with  
653 a new scoring function, efficient optimization, and multithreading. *Journal of Computational*  
654 *Chemistry*, 31(2):455–461, June 2009. ISSN 1096-987X. doi: 10.1002/jcc.21334. URL <http://dx.doi.org/10.1002/jcc.21334>.  
655
- 656 Haorui Wang, Marta Skreta, Cher-Tian Ser, Wenhao Gao, Lingkai Kong, Felix Strieth-Kalthoff,  
657 Chenru Duan, Yuchen Zhuang, Yue Yu, Yanqiao Zhu, Yuanqi Du, Alán Aspuru-Guzik, Kirill  
658 Neklyudov, and Chao Zhang. Efficient evolutionary search over chemical space with large lan-  
659 guage models, 2025. URL <https://arxiv.org/abs/2406.16976>.  
660
- 661 David Weininger. Smiles, a chemical language and information system. 1. introduction to methodol-  
662 ogy and encoding rules. *Journal of Chemical Information and Computer Sciences*, 28(1):31–36,  
663 1988. doi: 10.1021/ci00057a005. URL <https://doi.org/10.1021/ci00057a005>.  
664
- 665 Andrew D. White. The future of chemistry is language. *Nature Reviews Chemistry*, 7(7):457–458,  
666 May 2023. ISSN 2397-3358. doi: 10.1038/s41570-023-00502-0. URL <http://dx.doi.org/10.1038/s41570-023-00502-0>.  
667
- 668 Yaowei Zheng, Richong Zhang, Junhao Zhang, Yanhan Ye, Zheyang Luo, Zhangchi Feng, and  
669 Yongqiang Ma. Llamafactory: Unified efficient fine-tuning of 100+ language models, 2024.  
670 URL <https://arxiv.org/abs/2403.13372>.
- 671 Xiangxin Zhou, Xiwei Cheng, Yuwei Yang, Yu Bao, Liang Wang, and Quanquan Gu. Decomptt:  
672 Controllable and decomposed diffusion models for structure-based molecular optimization, 2024.  
673 URL <https://arxiv.org/abs/2403.13829>.  
674
- 675 Yiheng Zhu, Jialu Wu, Chaowen Hu, Jiahuan Yan, Chang-Yu Hsieh, Tingjun Hou, and Jian Wu.  
676 Sample-efficient multi-objective molecular optimization with gflownets, 2023. URL <https://arxiv.org/abs/2302.04040>.  
677

## 678

## 679 A ABFE SETUP

## 680

681 For our ABFE calculations, we utilize the following Binding Affinity Tool `BAT.py` Heinzelmann  
682 & Gilson (2021) repository: <https://github.com/GHeinzelmann/BAT.py>. We simulate  
683 using OpenMM and the standard SDR method. For calculations of molecules generated by docking  
684 as the oracle, we use the ligand pose generated by AutoDock as the starting pose for the calculation.  
685 For calculations of molecules generated by Boltz-2 as the oracle, we use the Boltz-2 predicted  
686 ligand pose as the starting pose. We separate the source of the poses to avoid potential bias toward  
687 one particular oracle in the ABFE calculation. Because Boltz-2 does not take a protein crystal  
688 structure as input and makes a prediction based on the given amino acid sequence, we first align the  
689 entire predicted Boltz-2 conformation to the protein crystal structure with ChimeraX Pettersen et al.  
690 (2020), then extract only the ligand pose for ABFE. We observe this alignment to yield an RMSE of  
691 under 0.7 angstroms; thus we are comfortable using the aligned ligand pose with the crystal structure  
692 in ABFE calculations. We do not observe frequent steric clashes resulting from this process.

693 Our simulation steps parameters for the `BAT.py` framework are as follows:  
694 `eq_steps1 = 500000` (Number of steps for equilibration gradual release)  
695 `eq_steps2 = 15000000` (Number of steps for equilibration after release)

696 `m_steps1 = 500000` (Number of steps per window for component m (equilibrium))  
697 `m_steps2 = 1000000` (Number of steps per window for component m (production))

698 `n_steps1 = 500000` (Number of steps per window for component n (equilibrium))  
699 `n_steps2 = 1000000` (Number of steps per window for component n (production))

700 `e_steps1 = 250000` (Number of steps per window for component e (equilibrium))  
701 `e_steps2 = 500000` (Number of steps per window for component e (production))

v\_steps1 = 500000 (Number of steps per window for component v (equilibrium))  
v\_steps2 = 1000000 (Number of steps per window for component v (production))

On 4 NVIDIA H200 GPUs, one ABFE calculation typically takes us around 16 hours to complete.

## B DIVERSITY IN BINDINGDB STARTING POPULATION

We very briefly analyze the diversity within the BindingDB starting population for c-MET and BRD4, in comparison to the diversity of the ZINC 250k starting population. In Table 5, we calculate the mean pairwise Tanimoto similarity for ZINC 250K, BindingDB for c-MET, and BindingDB for BRD4. Because the ZINC 250K starting population is just a random sample of 120 ligand from the entire set, we randomly sample from ZINC 250K 100 times to reduce variance.

Table 5: Starting population diversity for ZINC 250K vs BindingDB

Starting Population	Mean Pairwise Tanimoto Similarity
ZINC 250K	0.15
BindingDB (c-MET)	0.20
BindingDB (BRD4)	0.19

We observe a very minimal difference in mean pairwise similarity between ZINC 250K and the BindingDB samples. This indicates that our method involving Butina clustering is sufficient in creating a pool of molecules that are diverse enough for use as a starting population in MOLLEO.

## C ADDITIONAL LLM FINE-TUNING INFORMATION

### C.1 EXAMPLE LIGAND CHAIN ANALYSIS

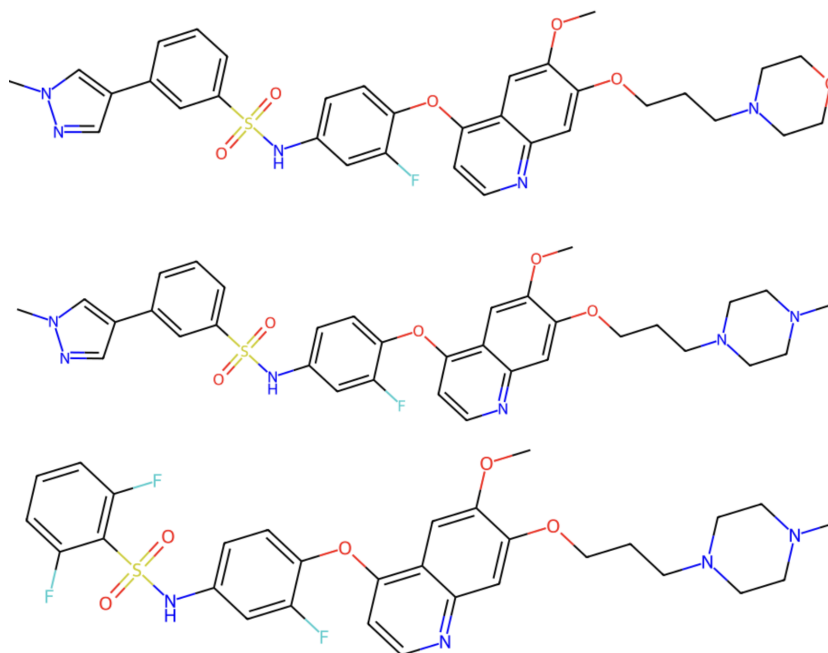
In this section, we briefly analyze a generated ligand chain for the c-MET target to provide further insight and transparency on the construction of the SFT dataset. The full chain of SMILES and corresponding experimental affinity is as follows:

- COc1cc2c(Oc3ccc(NS(=O)(=O)c4cccc(-c5cnn(C)c5)c4)cc3F)ccnc2cc1OCCCN1CCOCC1  
-7.859743051032407
- COc1cc2c(Oc3ccc(NS(=O)(=O)c4cccc(-c5cnn(C)c5)c4)cc3F)ccnc2cc1OCCCN1CCN(C)CC1  
-8.519634173245192
- COc1cc2c(Oc3ccc(NS(=O)(=O)c4c(F)cccc4F)cc3F)ccnc2cc1OCCCN1CCN(C)CC1  
-9.40241538421135
- COc1cc2c(Oc3ccc(NC(=O)C4(c5nnc(-c6ccc(F)cc6)o5)CC4)cc3F)ccnc2cc1OCCCN1CCCCC1  
-9.746740922094766
- COc1ccc(/C=N/NC(=O)Nc2ccc(Oc3ccnc4cc(OCCCN5CCOCC5)c(OC)cc34)c(F)c2)cc1  
-9.88726911173949
- CCC(=NNC(=O)Nc1ccc(Oc2ccnc3cc(OCCCN4CCCC4)c(OC)cc23)c(F)c1)c1cccc1  
-10.00374639143023
- COc1cc2c(Oc3ccc(NC(=O)NN=C(C)c4cccc4)cc3F)ccnc2cc1OCCCN1CCCCC1  
-10.116875164553585
- COc1ccc(-n2nc(C(=O)Nc3ccc(Oc4ccnc5cc(OCCCN6CCCC6)c(OC)cc45)c(F)c3)n(C)c2=O)cc1  
-10.218632169786542
- COc1cc2c(Oc3ccc(NC(=O)NN4C(=O)CSC4c4c(F)cccc4F)cc3F)ccnc2cc1OCCCN1CCCC1  
-10.256847106153646
- COc1cc2c(Oc3ccc(NC(=O)NS(=O)(=O)C4ccc(C)cc4)cc3F)ccnc2cc1OCCCN1CCOCC1  
-10.27692109634116

- 756 11. COc1cc2c(Oc3ccc(NC(=O)NN=Cc4ccc(Cl)cc4)cc3F)ccnc2cc1OCCCN1CCC(C)CC1  
757 -10.341580836295224
- 758 12. COc1cc2c(Oc3ccc(NC(=O)/C=C/S(=O)(=O)c4ccccc4OC)cc3F)ccnc2cc1OCCCN1CCCCC1  
759 -10.440497903230485
- 760 13. COc1cc2c(Oc3ccc(NC(=O)c4nn(-c5ccccc5Cl)c5cc(F)ccc5c4=O)cc3F)ccnc2cc1OCCCN1CCC(C)CC1  
761 -10.468043614008312
- 762 14. COc1cc2c(Oc3ccc(NC(=O)NN=Cc4ccc(F)cc4)cc3F)ccnc2cc1OCCCN1CCCCC1  
763 -10.527305631989824
- 764 15. COc1cc2c(Oc3ccc(NC(=O)Nc4nc5c(C)ccc(C)c5s4)cc3F)ccnc2cc1OCCCN1CCN(C)CC1  
765 -10.559320239451706
- 766 16. COc1cc2c(Oc3ccc(NC(=O)NS(=O)(=O)C4ccccc4)cc3F)ccnc2cc1OCCCN1CCOCC1  
767 -10.629062637222779
- 768 17. COc1cc2c(Oc3ccc(NC(=O)c4nnn(-c5ccccc5C)c4C)cc3F)ccnc2cc1OCCCN1CCC(C)CC1  
769 -10.708130046611966
- 770 18. COc1cc2c(Oc3ccc(NC(=O)c4nnn(-c5ccccc5C)c4C)cc3F)ccnc2cc1OCCCN1CCCCC1  
771 -10.75201130373146
- 772 19. COc1cc2c(Oc3ccc(NC(=O)c4nn(-c5ccc(F)cc5)c(=O)n4C)cc3F)ccnc2cc1OCCCN1CCC(C)CC1  
773 -10.850928370666724
- 774 20. COc1cc2c(Oc3ccc(NC(=O)c4nn(-c5cc(C)ccc5C)c5ccccc5c4=O)cc3F)ccnc2cc1OCCCN1CCOCC1  
775 -10.90736400619354
- 776 21. COc1cc2c(Oc3ccc(NC(=O)c4cc(-c5ccccc5)ccn4)cc3F)ccnc2cc1OCCCN1CCCCC1  
777 -10.944002041495516
- 778 22. COc1cc2c(Oc3ccc(NC(=O)c4nn(-c5ccc(Cl)cc5Cl)c5ccccc5c4=O)cc3F)ccnc2cc1OCCCN1CCCCC1  
779 -11.010603179910028
- 780 23. COc1cc2c(Oc3ccc(NC(=O)c4nn(-c5ccc(C)cc5)c5ccccc5c4=O)cc3F)ccnc2cc1OCCCN1CCOCC1  
781 -11.077708041026122
- 782 24. COc1cc2c(Oc3ccc(NC(=O)c4cn(-c5ccccc5Cl)nn4)cc3F)ccnc2cc1OCCCN1CCCCC1  
783 -11.14449718579243
- 784 25. COc1cc2c(Oc3ccc(NC(=O)NS(=O)(=O)C4ccc(F)cc4)cc3F)ccnc2cc1OCCCN1CCCCC1  
785 -11.229911129679115
- 786 26. COc1cc2c(Oc3ccc(NC(=O)c4c(Cl)c5ccccc5n(-c5ccc(F)cc5)c4=O)cc3F)ccnc2cc1OCCCN1CCOCC1  
787 -11.28329193813796
- 788 27. COc1cc2c(Oc3ccc(NC(=O)c4nnn(-c5ccccc5C(F)(F)F)c4C(F)(F)F)cc3F)ccnc2cc1OCCCN1CCN(C)CC1  
789 -11.3060688231394
- 790 28. COc1cc2c(Oc3ccc(NC(=O)c4nnn(-c5ccccc5C(F)(F)F)c4C)cc3F)ccnc2cc1OCCCN1CCOCC1  
791 -11.354432508931753
- 792 29. COc1cc2c(Oc3ccc(NC(=O)c4cc(-c5ccccc5)ccn4)cc3F)ccnc2cc1OCCCN1CCN(C)CC1  
793 -11.380181174324182
- 794 30. COc1cc2c(Oc3ccc(NC(=O)c4nn(-c5cccc(F)c5)c(=O)c5ccccc45)cc3F)ccnc2cc1OCCCN1CCCCC1  
795 -11.407100628036758
- 796 31. COc1cc2c(Oc3ccc(NC(=O)c4nnn(-c5ccccc5C(F)(F)F)c4C(F)(F)F)cc3F)ccnc2cc1OCCCN1CCOCC1  
797 -11.449923572095255
- 798 32. COc1cc2c(Oc3ccc(NC(=O)c4nnn(-c5ccccc5C(F)(F)F)c4C(F)(F)F)cc3F)ccnc2cc1OCCCN1CCCCC1  
799 -11.49608662779955
- 800 33. COc1cc2c(Oc3ccc(NC(=O)c4nn(-c5ccc(F)cc5)c5ccccc5c4=O)cc3F)ccnc2cc1OCCCN1CCC(C)CC1  
801 -11.546155255743054
- 802 34. COc1cc2c(Oc3ccc(NC(=O)c4nn(-c5cccc(C(F)(F)F)c5)c5ccccc5c4=O)cc3F)ccnc2cc1OCCCN1CCCCC1  
803 -11.600851900298952
- 804 35. COc1cc2c(Oc3ccc(NC(=O)c4c(C)n(-c5ccccc5Cl)c(=O)n4C)cc3F)ccnc2cc1OCCCN1CCN(C)CC1  
805 -11.640341597115352

- 810 36. COc1cc2c(Oc3ccc(NC(=O)c4nn(-c5ccccc5F)c5ccccc5c4=O)cc3F)ccnc2cc1OCCCN1CCC(C)CC1  
 811 -11.705001337069415
- 812 37. COc1cc2c(Oc3ccc(NC(=O)c4nnc(-c5ccccc5)c4C)cc3F)ccnc2cc1OCCCN1CCOCC1  
 813 -11.831464114782504
- 814 38. COc1cc2c(Oc3ccc(NC(=O)NS(=O)(=O)C4ccc(F)cc4)cc3F)ccnc2cc1OCCCN1CCCC1  
 815 -11.860354039531494
- 816 39. COc1cc2c(Oc3ccc(NC(=O)c4nnc(-c5ccccc5)c4C)cc3F)ccnc2cc1OCCCN1CCCC1  
 817 -11.99248313799697
- 818 40. COc1cc2c(Oc3ccc(NC(=O)c4cc(-c5ccc(C)cc5)ccn4)cc3F)ccnc2cc1OCCCN1CCN(C)CC1  
 819 -12.07155054738616
- 820 41. COc1cc2c(Oc3ccc(NC(=O)c4nc5ccccc5n(-c5ccccc5Cl)c4=O)cc3F)ccnc2cc1OCCCN1CCN(C)CC1  
 821 -12.162827172829553
- 822 42. COc1cc2c(Oc3ccc(NC(=O)c4nc5ccccc5n(-c5ccc(F)cc5)c4=O)cc3F)ccnc2cc1OCCCN1CCN(C)CC1  
 823 -12.333171207662138

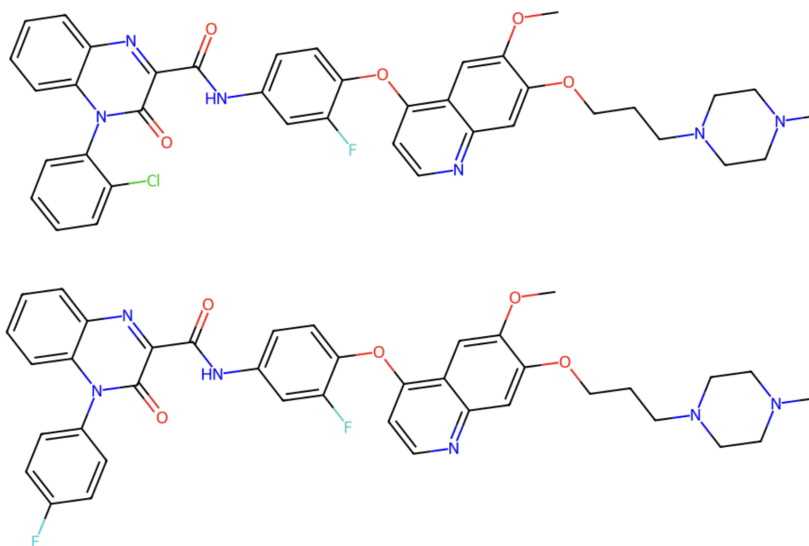
826 We can immediately observe that all ligands are relatively similar in structure and arrangement,  
 827 and that the experimental affinity gradually (an unconditionally) improves as the chain progresses.  
 828 Figure 5 shows what a modifications from one molecule in the chain to the next looks like, showing  
 829 the first three ligands from this chain. We can very clearly see the minimal, single change that  
 830 occurs at every step. From ligand 1 to ligand 2, the terminal heterocycle on the far right changes  
 831 from containing one oxygen and one nitrogen to containing two nitrogens and a methyl group. From  
 832 ligand 2 to ligand 3, the leftmost group is dropped and additional fluorines are added. It is crucial  
 833 that changes are minimal and realistic, as we want an LLM to be able to rationalize any of the  
 834 changes in a few interpretable steps.



859 Figure 5: Visualizations of the first 3 ligands in this example chain. Observe how modifications are  
 860 gradual and resemble changes that might derive from a legitimate reasoning process.

862 Figure 6 further demonstrates this by showing the final two ligands from this chain. The similarities  
 863 to the initial ligands are clear, and one can imagine how the gradual steps along the chain may have  
 led to these significant changes. Crucially, even here, we can observe minimal changes being made.

864  
865  
866  
867  
868  
869  
870  
871  
872  
873  
874  
875  
876  
877  
878  
879  
880  
881  
882



883 Figure 6: Visualizations of the last 2 ligands in this example chain. Notice the obvious similarities  
884 to the start of the chain, and notice how changes are still minimal and gradual here.

885  
886  
887  
888  
889  
890  
891  
892

According to the affinities from the chain, these two ligands have experimental affinities of over -12 kcal/mol, while the starting molecules had affinities hovering around -8 kcal/mol. From this, we can directly visualize how these ligand chains might guide an LLM toward more informed modifications of ligands; each change is gradual and reasonable, yet at the same time gradually progressing the desired binding affinity.

893  
894  
895

## C.2 LLM PROMPTS FOR DATASET FORMATION

896  
897  
898

This section provides the exact prompts used to create the supervised fine-tuning dataset used in this work.

899  
900  
901  
902

Consider one of the ligand chains formed by the clustering-sorting process. For each ligand/position in the chain, we first ask the LLM to generate a summary based on all the past (weaker affinity) ligands in the chain. This summary is used in the input for SFT, simulating the information the LLM might receive for an optimization step.

903

Prompt to generate the summary of past ligand modifications used in the input for SFT

904  
905  
906  
907  
908  
909  
910  
911  
912  
913  
914  
915

You are a chemistry-aware assistant that is collaborating with me on generating a ligand for a protein with high binding affinity. Below is a chronological history of past ligands you've generated. Provide a summary of changes and modifications you've made so far in regards to the ligand structure and how it impacts the binding affinity; the goal is to give context about past iterations to another agent. Be sure to explicitly output the SMILES of every past ligand. Do not provide any suggestions for future generations at this time. Keep your response relatively short.  
SMILES: *Affinity*  
SMILES: *Affinity*  
SMILES: *Affinity*  
...

916  
917

Where we input all previous ligands and their binding affinities in the chain as *SMILES: Affinity*. The generated summary is placed into the following format, which becomes the full input for SFT:

918  
919  
920  
921  
922  
923  
924  
925  
926  
927  
928  
929  
930  
931

#### Full SFT Input

We are collaborating on generating a ligand for a protein with high binding affinity. I will give you the output from docking software after each of your attempts. Provided below is a brief summary of past ligand modifications:

\*\*\*\**GENERATED SUMMARY*\*\*\*\*

First describe what you have learned from the above summary. Then based on that knowledge, generate a ligand that can bind to this protein with high binding affinity. Ensure that your generation is unique and is not found within the provided data. Follow this format for your final answer:  $\boxed{\text{MOLECULE}}$ , where MOLECULE is your proposed ligand in SMILES format.

*SMILES: Affinity*

*SMILES: Affinity*

*SMILES: Affinity*

...

932  
933  
934  
935

After this, we ask the LLM to generate reasoning that might lead an agent to generate the next (stronger affinity) ligand in the chain. This becomes the full desired output for SFT. In essence, we want to tune the model to carry out what we know to be a strong modification decision for a particular protein target based off information provided in the input.

936  
937

#### Prompt to generate the full output for SFT:

We are collaborating on generating a ligand for a protein with high binding affinity. I will give you the output from docking software after each of your attempts. Provided below is a brief summary of past ligand modifications:

\*\*\*\**GENERATED SUMMARY*\*\*\*\*

Based on the summary, first pretend that you are thinking about what modifications to make to create a stronger molecule. In the end, choose to generate the molecule *NEXT\_LIGAND*. Do not mention this molecule until you've explained what decisions and specific structural modifications would lead to this new molecule. It's crucial that you pretend to have come up with this generation yourself after some brief analysis of the provided summary. Provide the final ligand explicitly in this exact format, character by character:  $\boxed{\text{NEXT\_LIGAND}}$ . Keep your response relatively short.

*SMILES: Affinity*

*SMILES: Affinity*

*SMILES: Affinity*

...

953

954

955

956

957

958

959

960

Notice that the first half of this prompt is the same as the actual input for SFT. However, we instead tell the LLM to pretend like it's doing the generation action, using the predetermined *NEXT\_LIGAND* as the guide for its explanation, where *NEXT\_LIGAND* is the next (higher affinity) ligand in the ligand chain. This results in an SFT output that not only contains the desired next ligand, but also provides a sample explanation for how you might modify previous ligands to create the new one. This is precisely what we want for the SFT dataset, as we want a model to learn how to make the best modifications for any given input to optimize toward a point of higher affinity. Here is a sample LLM output for this prompt:

961

#### Sample Full SFT Output

Considering the previous ligand's balance of hydrophobic aromatic rings, heterocycles, and hydrogen-bonding groups, I think introducing a more rigid and cyclic structure could enhance binding affinity. Replacing flexible linker regions with nitrogen-containing heterocycles might improve interactions through additional hydrogen bonds and electrostatic contacts. Additionally, modifying substituents to include carbonyl groups could further strengthen hydrogen bonding capacity. Incorporating a carbamate moiety at a strategic position can also influence binding strength. After analyzing these features, I realize that a cyclic structure incorporating these elements—specifically, a fused ring system with carbamate and aromatic groups—optimize interactions with the protein binding site. Therefore, I plan to generate a ligand with these features, resulting in the target molecule:  $\boxed{\text{NEXT\_LIGAND}}$ .

970  
971

### C.3 SFT TRAINING PROCESS

In this section, we provide information about the training process for our supervised fine-tuned model. We fine-tune using the unified open-source fine-tuning repository LLaMA-Factory Zheng et al. (2024). We utilize Low-Rank Adaption (LoRA) Hu et al. (2021) to train a subset of the model parameters, saving a significant amount of time and computation. We utilize all default hyperparameters from the LLaMA-Factory repository (see the llama3\_lora\_sft.yaml example file in examples/train\_lora/), except for modifying the train-validation split to be 0.95/0.05 instead of 0.90/0.10.

Figure 7 provides the training and validation loss graphs for this process for the BRD4 target. We train for 10 epochs on a dataset of around 5,000 samples, taking around 150 minutes on a NVIDIA H200. As is evident from the figure, validation loss drops rapidly, then rather quickly plateaus, and increases rapidly as the model overfits to the relatively small dataset. We let the training continue past the overfitting point just for the chance of any emergent behavior. However, we carefully select the checkpoint for which the validation loss is at its minimum, which we evaluate to be the checkpoint at step 2,000. We merge the LoRA adapters at this checkpoint into the original base model to obtain the fine-tuned model used in MOLLEO optimization.

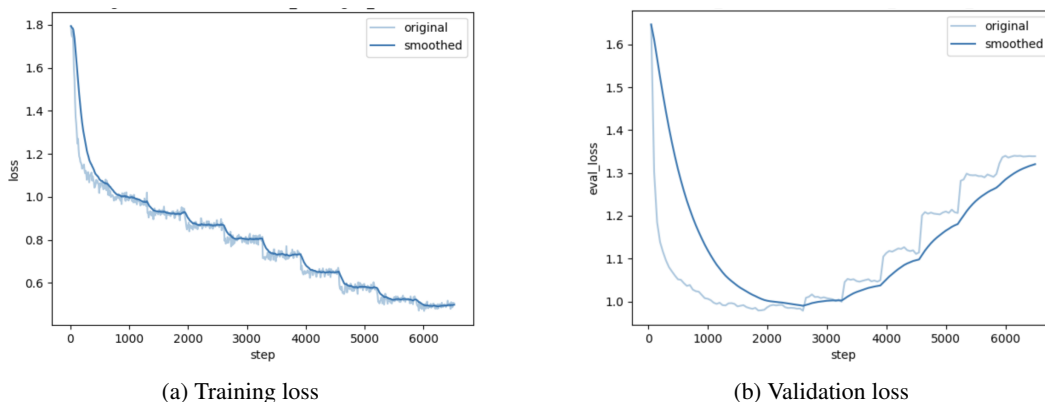


Figure 7: Training and validation loss graphs for supervised fine-tuning

### C.4 FURTHER COMPARISON OF TUNED VS UNTUNED LLAMA

In this section, we further compare the results of our fine-tuned Llama model with the untuned model. Specifically, we account for the high amount of invalid format responses that the untuned model yields in order to provide a more focused comparison of the generated molecules themselves.

We do this by only considering the first  $n$  LLM generations of the fine-tuned model, where  $n$  is the total number of validly-formatted responses made by the untuned model throughout the entire 1000-step process. In this way, we take the generation results from an equal number of valid LLM attempts from both models, allowing us to purely compare the quality of molecule generations between the models without statistical interference from answers with invalid formats. The results from this limitation are shown in Table 6:

Table 6: Boltz-2 affinity (kcal/mol) for untuned Llama vs fine-tuned Llama w/ limitation applied

Method	Mean $\pm$ SD (c-MET)	Mean $\pm$ SD (BRD4)
Untuned Llama	-10.8 $\pm$ 0.4	-10.7 $\pm$ 0.7
Fine-tuned Llama w/ limitation	<b>-11.1 <math>\pm</math> 0.3</b>	<b>-10.9 <math>\pm</math> 0.3</b>

With this limitation, the fine-tuned model yields  $p = 0.02$  for c-MET and  $p = 0.15$  for BRD4. However, we can consider a joint probability for the hypothesis that the fine-tuning method improves generations across all targets, since the runs are entirely independent. Using Fisher’s method with 4 degrees of freedom, we get a joint probability of  $p_{combined} \approx 0.02$ , giving us statistically significant

evidence that our fine-tuning framework improves the inherent generation quality of the LLM for any protein target  $p$ .

This limitation is actually heavily biased toward the untuned model, since its model generations are built upon existing strong molecules generated by default crossover/mutation operators throughout the entire course of the optimization process, while the fine-tuned results are limited only to the initial parts of the optimization process. Even with such a limiting ablation, we observe a statistically significant increase in binding affinity with the fine-tuned model, concretely supporting the claim that our post-training framework improves the inherent quality of molecule generations within the optimization process.

## D DEMONSTRATION FOR LACK OF BINDINGDB LIGANDS

In this section, we demonstrate that for our supervised fine-tuning dataset, we have a workaround in the situation where we are optimizing for a protein target that is not well studied and has few results for experimentally-tested ligand binders.

Our original dataset for c-MET was sufficiently large because c-MET is a very well-studied target. As a proof of concept however, we pretended that this was not a well-studied target, and instead formed our dataset by considering 20 protein targets that we determined to have structural similarities c-MET using the BLASTP tool Altschul et al. (1990). We took the ligand entries corresponding to these 20 targets and applied the same process to form a surrogate dataset. We trained the same small Llama model on this dataset, and its performance in MOLLEO is shown in Table 7.

Table 7: Boltz-2 affinity (kcal/mol) for Llama tuned on 2.5k vs 30k datasets for c-MET

Method	Mean $\pm$ SD
Llama	-10.8 $\pm$ 0.4
Llama (c-MET dataset)	-11.7 $\pm$ 0.1
Llama (surrogate dataset)	-11.6 $\pm$ 0.2

Comparing the results we get from a model trained on the pure c-MET dataset against our surrogate dataset, we get  $p = 0.13$  from a two-sided independent Student’s t-test, which implies a non-significant difference. We see that if the desired protein target does not have sufficient ligand entries, we can make up for it by identifying protein targets that are structurally similar to it and use their ligand entries instead. This guarantees some level of similarity in the input ligands, and as demonstrated experimentally, does not hurt performance relative to using a dataset comprised only of target-specific ligands.